BULLETIN OF THE
KOREAN CHEMICAL SOCIETY

VOLUME 4, NUMBER 3, JUNE 20, 1983

Calculation of NMR Shift in Paramagnetic System When the Threefold Axis is Chosen as the Quantization Axis (I). The NMR Shift for a $3d^1$ System in a Strong Crystal Field of Octahedral Symmetry

Sangwoon Ahn† and Euisuh Park

Department of Chemistry, Jeonbug National University, Jeonju 520, Korea

Kee Hag Lee

Department of Chemistry, Won Kwang University, Iri 510, Korea,
(Received October 13, 1982).

The NMR shift arising from the electron angular momentum and the electron spin dipolar–nuclear spin angular momentum interaction has been examined for a $3d^1$ system in a strong octahedral crystal field when the threefold axis is chosen as the quantization axis. To investigate the NMR shift in this situation, first, we have extended the evaluation of the hyperfine integrals to any pairs of 3d orbitals adopting a general method which is applicable to a general vector R, pointing in arbitrary direction in space. Secondly, a general expression using a nonmultipole technique is derived for the NMR shift resulting from the electron angular momentum and the electron spin dipolar–nuclear spin angular momentum interactions. From this expression all the multipolar terms are determined. $\Delta B/B$ for the $3d^1$ system in this case is compared with that for the $3d^1$ system when the z axis is chosen as the quantization axis. When we choose the threefold axis as the quantization axis, it is found that along the ⟨100⟩, ⟨010⟩ and ⟨001⟩ axes, $\Delta B/B$ values are significantly different from each other and along the ⟨111⟩, ⟨-1-1-1⟩, ⟨-11-1⟩, ⟨1-11⟩, ⟨-1-11⟩, ⟨11-1⟩, ⟨1-1-1⟩ and ⟨-111⟩ axes, $\Delta B/B$ values are however the same. We also find that the $1/R^7$ term contributes dominantly to the NMR shift for all values of R. When $1/R^5$ term is included, there is good agreement between the exact solution and the multipolar terms when $R \leqslant 0.35$ nm.

Introduction

Since the early 1960 a great deal of interest has been concentrated on the NMR shift arising from $3d^n$ system. The NMR shift has been classified as arising both the Fermi contact and the pseudo contact mechanisms. In specific cases one of these mechanisms may dominate. For example, the NMR shift in transition metal complexes[1] has been interpreted as arising dominantly through the Fermi contact mechanism. For this case, a generalized expression for the NMR shift for $3d^n$ system was derived[2]

$$\frac{\Delta B}{B} = -\frac{\mu_B}{3g_N\mu_N}\left\{\frac{2}{\lambda}\frac{(g-K)(g-2)}{(2-K)} + (g-K)g\frac{J(J+1)}{kT}\right\}$$
$$g = 1 + \{J(J+1) - L(L+1) + S(S+1)\}/2J(J+1) \quad (1)$$
$$\lambda = \pm\zeta/2S$$

Here ζ is the spin–orbit coupling constant and only the $^{(2s+1)}T_2$ ground state has been considered with bonding effects by using the orbital reduction factor K.

In other situations the interpretation has been based on a dominant pseudo contact contribution to the NMR shift[3]. However, it was reported that, in a more detailed treatment of NMR shifts, both mechanisms should be considered[4]. The pseudo contact NMR shift was first given by McConnell and Robertson[5], adopting the dipolar approximation, in the form

$$\frac{\Delta B}{B} = -\mu^2{}_B\frac{S(S+1)}{3kT}\frac{(3\cos^2\theta - 1)}{R^3}F(g) \quad (2)$$

where R is the distance between the NMR nucleus and the electron bearing nucleus and $F(g)$ is a function of the princi-

pal g-value. Kurland and McGravey extended this work and showed that the pseudo contact shift may be expressed in terms of the magnetic susceptibility components, $\chi_{\alpha\alpha}$, namely

$$\frac{\Delta B}{B}=-\frac{1}{3R^3}\left\{\left[\chi_{zz}-\frac{1}{2}(\chi_{xx}+\chi_{yy})\right](3\cos^2\theta-1)+\frac{3}{2}(\chi_{xx}-\chi_{yy})\sin^2\theta\cos\phi\right\} \quad (3)$$

This expression has been used extensively in interpreting the pseudo contact contribution to NMR shifts in paramagnetic molecules. Buckingham and Stiles[7] proposed that molecular magnetic multipoles higher than dipole may contribute significantly to the neighbor-anisotropy shift in nuclear magnetic spectroscopy. In the notation of Stiles the NMR shift may be expressed as

$$\frac{\Delta B}{B}=\sum_{L=2}^{K}\sum_{M=0}^{L}(A_{LM}\cos M\phi+B_{LM}\sin M\phi)\,P^M(\cos\theta)/R^{L+1} \quad (4)$$

where $K=2(2l+1)$ for a specific l-electron, $P_L{}^M(\cos\theta)$ the associated Legendre polynomials, the coefficients A_{LM} and B_{LM} measure the anisotropy in the multipolar magnetic susceptibilities of the molecule. Recently attention has been focused on the exact solution of the NMR shift arising from the elctron angular monentum and the electron spin dipolar-nuclear spin angular momentum interactions[8], including the multipolar terms. This method (nonmultipole expansion method) has been applied to calculate the NMR shifts for $3d^1$ system in a strong crystal field of octahedral, tetragonal and trigonal symmetries and $4f^1$ system in an octahedral crystal field[9] when the z axis is chosen as the quantization axis.

The purpose of this work is, first, to extend the evaluation of the hyperfine integrals to any pairs of d orbitals which are required to investigate the NMR shift for d^n system in a strong crystal field of octahedral and trigonal symmetries when the threefold axis is chosen as the quantization axis, and secondly, to develop a method for calculating the NMR shift for a $3d^1$ system in a strong crystal field of octahedral symmetry when the threefold axis is chosen as the quantization axis, adopting the nonmultipole expansion method. The calculated results are compared with those for a $3d^1$ system when the z axis is chosen as the quantization axis. The NMR results are also separated to the contributions of $1/R^5$ and $1/R^7$ terms and are compared with the multipolar NMR shifts ($1/R^5$ and $1/R^7$ represent the quadrupolar and octapolar terms, respectively).

2. Theory

The hamiltonian representing the various interactions may be expressed as

$$\mathcal{H}=-\frac{h^2}{2m_e}\nabla^2-\frac{Ze^2}{4\pi e_0 r}+V(r)+\zeta\,\boldsymbol{l}\cdot\boldsymbol{s}+\mu_B(\boldsymbol{l}+2\boldsymbol{s})+\mathcal{H}_H \quad (5)$$

where V(r) is a crystal field term and

$$\mathcal{H}_H=\frac{\mu_0}{4\pi}g_N\mu_B\mu_N\left\{\frac{2\boldsymbol{l}_N\cdot\boldsymbol{I}}{r_N{}^3}+g_s\left[\frac{3(\boldsymbol{r}_N\cdot\boldsymbol{s})\boldsymbol{r}_N\cdot\boldsymbol{I}}{r_N{}^5}-\frac{\boldsymbol{S}\cdot\boldsymbol{I}}{r_N{}^3}\right]\right\} \quad (6)$$

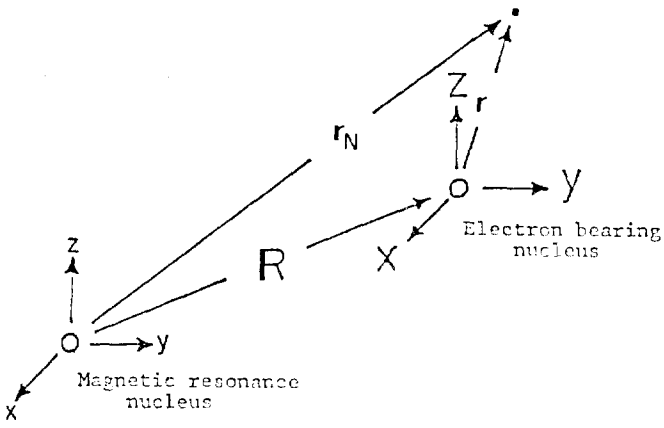

Figure 1. The coordinate system for calculation of the NMR shift.

Here r and r_N are electron radius vector about the electron-bearing atom and nucleus with spin angular momentum, I, respectively. The quantity B is the applied magnetic field and the other terms have their usual meaning as shown in Figure 1.

If the threefold axis is chosen as the quantization axis, the axial wave functions with t_2 symmetry take, in $|m^{\pm}>$ notation, the following form[10]

$$\begin{aligned}\phi^{\pm}{}_0&=|3dz^{2\pm}>\\ \phi^{\pm}{}_1&=\sqrt{\frac{2}{3}}\,|2^{\pm}>-\sqrt{\frac{1}{3}}\,|-1^{\pm}>\\ \phi^{\pm}{}_2&=\sqrt{\frac{2}{3}}\,|-2^{\pm}>+\sqrt{\frac{1}{3}}\,|1^{\pm}>\end{aligned} \quad (7)$$

If the imaginary 3d orbitals are transformed to the real 3d orbitals, the axial wave functions with the threefold axis to be our axis of quantization are

$$\begin{aligned}\phi_0{}^{\pm}&=|3d_{z^2}{}^{\pm}>\\ \phi_1{}^{\pm}&=\sqrt{\frac{1}{3}}\,|3d_{z^2-y^2}{}^{\pm}>+\sqrt{\frac{1}{3}}i\,|3d_{xy}{}^{\pm}>-\sqrt{\frac{1}{6}}\,|3d_{xz}{}^{\pm}>\\ &\quad+\sqrt{\frac{1}{6}}i\,|3d_{yz}{}^{\pm}>\\ \phi^{\pm}{}_2&=\sqrt{\frac{2}{3}}\,|3d_{x^2-y^2}{}^{\pm}>-\sqrt{\frac{1}{3}}i\,|3d_{xy}{}^{\pm}>-\sqrt{\frac{1}{6}}\,|3d_{xz}{}^{\pm}>\\ &\quad-\sqrt{\frac{1}{6}}i\,|3d_{yz}{}^{\pm}>\end{aligned} \quad (8)$$

A $3d^1$ system in a strong octahedral crystal field results in a $^2T_2$ ground state. The spin-orbit coupling interactions result in a splitting of the $^2T_2$ ground state into the $|^2T_2U'c>$ and $|^2T_2E''c>$ eigenfunctions[11] with relative eigenvalues $-\zeta/2$ and ζ, respectively. The magnetic field interaction is treated as a perturbation yielding six eigenfunctions ϕ_n with eigenvalues E_n. We derive a general expression to calculate the magnetic moment for $3d^1$ complexes when the threefold axis is chosen to be our axis of quantization. It may be written as

$$\mu=\left\{\frac{3x-8[1-\exp(3x/2)]}{[1+2\exp(3x/2)]}\right\} \quad (9)$$

with $x=\zeta/kT$

It is interesting to note that this expression (Eq. 9) is exactly

the same form as for the case when the z axis is chosen as the quantization axis. To determine the NMR shift the principal values σ_{xx}, σ_{yy} and σ_{zz} of the NMR screening tensor σ are determined by considering the magnetic field interaction as parallel to the x, y and z axes and averaged assuming a Boltzmann distribution. The contribution to the NMR shift, ΔB, is given by

$$\Delta B = B(\sigma_{xx}+\sigma_{yy}+\sigma_{zz})/3 \tag{10}$$

where

$$\sigma_{\alpha\alpha} = \left(\frac{\partial^2 <\mathcal{H}_H>}{\partial\mu_\alpha \partial B_\alpha}\right)_{\mu=B=0} \tag{11}$$

with

$$\mu = g_N \mu_N \boldsymbol{I}$$

The term $<\mathcal{H}_H>$ refers to the Boltzmann average of the hyperfine interaction represented by equation(6).

The Evaluation of the Hyperfine Integrals

To calculate the hyperfine interactions, it is necessary to evaluate the hyperfine integrals involving the dipolar hyperfine interaction and the electron angular momentum interaction represented by equation (6). It should be stressed that the hyperfine integrals have previously been evaluated for the special case where R lies along the z axis using a method given by McConnel and Strathdee[12] in 1959. The operator was expressed as a function of $\boldsymbol{R}$ and $\boldsymbol{r}_N$ and the integration performed in the O_{xyz} system. The singular nature of the operator at the magnetic resonance nucleus causes problems with this method. This method of evaluating the hyperfine integrals has been employed by various rese archers in predicting chemical shifts[13,14].

Recently a general method which is applicable to a general vector R, pointing in any direction in space has been developed by Golding and Stubbs[8]. In this method, the integrand is expressed as a function of $\boldsymbol{R}$ and $\boldsymbol{r}_N$ using the transformation

which will be given in the following, and then the integration is performed in the $O_N x_N y_N z_N$ system. We adopt this method to evaluate the hyperfine integrals involving any pairs of 3d orbitals. As far as we are aware, the evaluation of the hyperfine interaction integrals for each pair of $3d_{xz}$, $3d_{xy}$ and $3d_{yz}$ orbitals has been performed.

In addition to the hyperfine interaction integrals for each pair of $3d_{xz}$, $3d_{xy}$ and $3d_{yz}$, it is required to evaluate the hyperfine integrals for all piars of 3d orbitals to investigate the NMR shift for $3d^n$ systems in a strong crystal field of octahedral and trigonal symmetries when the threefold axis is chosen as the quantization axis. Here we choose the Slater type orbitals of the form

$$\phi_{lm} = Nr^l \exp(-\beta r)\ Y_{lm}(\theta,\phi) \tag{12}$$

The electronic wave functions in real notation for the 3d orbitals are

$$3d_{xz} = (2\beta^7/3\pi)^{\frac{1}{2}}\, xz \exp(-\beta r)$$

$$3d_{yz} = (2\beta^7/3\pi)^{\frac{1}{2}}\, yz \exp(-\beta r)$$

$$3d_{xy} = (2\beta^7/3\pi)^{\frac{1}{2}}\, xy \exp(-\beta r)$$

$$3d_{z^2} = (\beta^7/18\pi)^{\frac{1}{2}}(3z^2-r^2)\exp(-\beta r)$$

$$3d_{x^2-y^2} = (\beta^7/6\pi)^{\frac{1}{2}}(x^2-y^2)\exp(-\beta r) \tag{13}$$

The hyperfine interaction integrals are evaluated by expressing the electron coordinate system O_{xyz} using the following identities[15],

$$r^l\, Y_{lm}(\theta,\phi) = \sum_{l_1=0}^{l}\sum_{l_2=0}^{l}\sum_{m_1=-l_1}^{l_1}\sum_{m_2=-l_2}^{l_2}(-1)^{l_1}\delta(l_1+l_2,\delta) \times\left\{\frac{4\pi(2l+1)!}{(2l_1+1)!(2l_2+1)!}\right\}^{\frac{1}{2}} <l_1 l_2 m_1 m_2 | l_1 l_2 l m> \times R^{l_1} Y_{l_1 m_1}(\Theta,\Phi)\, r_N{}^{l_2} Y_{l_2 m_2}(\theta_N,\phi_N) \tag{14}$$

$$\exp(-\beta r) = 4\sum_{n=0} b_n(\boldsymbol{R},\boldsymbol{r}_N)\sum_{h=-n} Y^*_{nh}(\Theta,\Phi)\, Y_{nh}(\theta_N,\phi_N) \tag{15}$$

where

$$b_n(\boldsymbol{R},\boldsymbol{r}_N) = (r_</r_>)^{\frac{1}{2}} I_{n+\frac{1}{2}}(2\beta r_<)\ K_{n+\frac{3}{2}}(2\beta r_>) - (r_</r_>)^{\frac{1}{2}} I_{n-\frac{1}{2}}(2\beta r_<)\ K_{n+\frac{1}{2}}(2\beta r_>) \tag{16}$$

where $r_<$ is the smaller of the pair $\boldsymbol{R}$, $\boldsymbol{r}_N$, and $r_>$ is the larger of $\boldsymbol{R}$, $\boldsymbol{r}_N$ and I_v and K_v are the modified Bessel functions.

(a) The Integrals of $l_{N\alpha}/r_N{}^3$

In order to evaluate the hyperfine integrals arising from the electron angular momentum-nuclear spin interaction, it is necessary to evaluate the following two center integrals

$$<\phi_{lm'}|\, l_{N\alpha}/r_N{}^3 |\phi_{lm}>$$

where

$$l_N = -i\hbar\, \boldsymbol{r}_N \times \nabla_N$$

To evaluate the above two center integral, the 3d orbitals are expressed as a function of the corrdinates of $\boldsymbol{R}$ and $\boldsymbol{r}_N$. As an example, the $3d_{z^2}$ which is expressed as a function of $\boldsymbol{R}$ and $\boldsymbol{r}_N$ takes the form,

$$|3d_{z^2}> = (\beta^7/18\pi)^{\frac{1}{2}}[2(z_N-Z)^2-(x_N-X)^2-(y_N-Y)^2] \times\exp[-\beta\{(z_N-Z)^2+(x_N-X)^2+(y_N-Y)^2\}^{1/2}] \tag{17}$$

where X,Y and Z are the components of vector $\boldsymbol{R}$ and x_N, y_N and z_N the components of vector $\boldsymbol{r}_N$ in Figure 1. Then the differentiation is performed. The net result is that

$$\phi^*_{lm'}(-i\hbar \boldsymbol{r}_N \times \nabla_N / r_N{}^3)\phi_{lm} = N^2\left\{f^{(l)}_{m'm}(\boldsymbol{R},\boldsymbol{r}_N)\, e^{\frac{-2\beta r}{r}} + g^{(l)}_{m'm}(\boldsymbol{R},\boldsymbol{r}_N)\, e^{-2\beta r}\right\}/r_N{}^3 \tag{18}$$

where $f^{(l)}_{m'm}$ and $g^{(l)}_{m'm}$ are homogenous polynomials of the cartesian coordinates $\boldsymbol{R}$ and $\boldsymbol{r}_N$ and are of degree $(2l+1)$ and

$2l$, respectively[16].

The two center integral is therefore transformed to the following form

$$\langle\phi_{lm'}|l_{N\alpha}/r_N{}^3|\phi_{lm}\rangle = N^2\int_0^\infty \frac{dx_N\,dy_N\,dz_N}{r_N{}^3}\left[f^{(l)}_{m'm}(\boldsymbol{R},\boldsymbol{r}_N)\frac{e^{-2\beta r}}{r}+g^{(l)}_{m'm}(\boldsymbol{R},\boldsymbol{r}_N)e^{-2\beta r}\right] \quad (19)$$

The integral $\langle\phi_{lm'}|l_{N\alpha}/r_N{}^3|\phi_{lm}\rangle$, where $|\phi_{lm'}\rangle$ and $|\phi_{lm}\rangle$ are real wave functions, is a purely imaginary quantity and is equal to

$$\frac{1}{2}\langle\phi_{lm'}|l_{N\alpha}/r_N{}^3|\phi_{lm}\rangle-\frac{1}{2}\langle\phi_{lm}|l_{N\alpha}/r_N{}^3|\phi_{lm'}\rangle$$

The integral involving $\exp(-2\beta r)/r$ vanishes in equation (19). The remaining integrals may be written as

$$\langle\phi_{lm'}|l_{N\alpha}/r_N{}^3|\phi_{lm}\rangle=\frac{N^2}{2}\int_0^\infty\int_0^{2\pi}\int_0^\pi \exp(-2\beta r)\left[g^{(l)}_{m'm}(\boldsymbol{R},\boldsymbol{r}_N)+g^{(l)}_{mm'}(\boldsymbol{R},\boldsymbol{r}_N)\right]\frac{dr_N}{r_N}\sin^2\theta_N\,d\theta_N\,d\phi_N \quad (20)$$

Using the following identities[17],

$$x=\left(\frac{2\pi}{3}\right)^{\frac{1}{2}}r[Y_{1-1}(\theta,\phi)-Y_{11}(\theta,\phi)]$$
$$y=\left(\frac{2\pi}{3}\right)^{\frac{1}{2}}ir[Y_{1-1}(\theta,\phi)+Y_{11}(\theta,\phi)]$$
$$z=\left(\frac{4\pi}{3}\right)^{\frac{1}{2}}r\,Y_{10}(\theta,\phi) \quad (21)$$

and the relationship[18]

$$Y_{l_1m_1}Y_{l_2m_2}=\sum_{l=l_1-l_2}^{l_1+l_2}\sum_{m=-l}^{l}(-1)^m\left\{\frac{(2l_1+1)(2l_2+1)(2l+1)}{4\pi}\right\}^{\frac{1}{2}}\times\begin{pmatrix}l_1 & l_2 & l\\ 0 & 0 & 0\end{pmatrix}\begin{pmatrix}l_1 & l_2 & l\\ m_1 & m_2 & m\end{pmatrix}Y_{l-m} \quad (22)$$

the homogenous polynomials, $g^{(l)}_{mm'}$, and $g^{(l)}_{m'm}$, are expanded in terms of a sum of products of the homogenous polynomials,

$$g^{(l)}_{mm'}=\sum_{L_1,L_2}\sum_{M_1,M_2}C_{m'm}(L_1,M_1;L_2,M_2)\,Y_{L_1M_1}(\Theta,\Phi)\,Y_{L_2M_2}(\theta_N,\phi_N) \quad (23)$$

where the $C_{m'm}(L_1, M_1; L_2, M_2)$ are functions of $\boldsymbol{R}$ and $\boldsymbol{r}_N$. Next, the exponential part $\exp(-2\beta r)$ is translated using equation (14).

Finally the integral may be written as

$$\langle\phi_{lm'}|l_{N\alpha}/r_N{}^3|\phi_{lm}\rangle=N^2\sum_{L_1,L_2}\sum_{M_1,M_2}\sum_{n=0}^{\infty}\int_0^\infty C_{mm'}(L_1,M_1;L_2,M_2)\,b_n(\boldsymbol{R},\boldsymbol{r}_N)\frac{d\,r_N}{r_N}\times\sum_{h=-n}^{n}Y^*_{n'n}(\Theta,\Phi)\,Y_{L_1M_1}(\Theta,\Phi)\times\int_0^\pi\int_0^{2\pi}Y_{nh}(\theta_N,\phi_N)\,Y_{L_2M_2}(\theta_N,\phi_N)\sin\theta_N\,d\theta_N\,d\phi_N \quad (24)$$

where the radial and angular parts have now been separated. Using the formula[19],

$$\int_0^\pi\int_0^{2\pi}Y_{l_1m_1}\,Y_{l_2m_2}\,Y_{l_3m_3}\sin\theta_N\,d\theta_N\,d\phi_N=\left\{\frac{(2l_1+1)(2l_2+1)(2l+1)}{4\pi}\right\}^{\frac{1}{2}}\begin{pmatrix}l_1 & l_2 & l_3\\ 0 & 0 & 0\end{pmatrix}\begin{pmatrix}l_1 & l_2 & l_3\\ m_1 & m_2 & m_3\end{pmatrix} \quad (25)$$

selection rules are obtained on n and h resulting in only a finite number of terms in the infinite sum being nonzero.

The evaluated integrals of $l_{N\alpha}/r^3$ are listed in appendix.

(b) The Dipolar Integrals

The hamiltonian representing the dipolar hyperfine interaction may be expressed in dyadic notation as

$$\mathcal{H}_D=\frac{\mu_0}{4\pi}g_S g_N\mu_B\mu_N\,\boldsymbol{S}\cdot\boldsymbol{T}\cdot\boldsymbol{I} \quad (26)$$

where $\boldsymbol{T}$ is a symmetric tensor whose components are given by

$$T_{\alpha\beta}=(3r_{N\alpha}r_{N\beta}-r^2{}_N\delta_{\alpha\beta})/r_N{}^5$$

Essentially, in calculating the dipolar integral, it is necessary to consider integrals of the form

$$\langle\phi_{lm'}|T_{\alpha\beta}|\phi_{lm}\rangle$$

We adopt a new approach which lead itself more readily to performing the calculation of these integrals in analytical form using a digital computer.

The angular wave functions are expressed as a function of the cartesian coordinate of $\boldsymbol{R}$ and $\boldsymbol{r}_N$ and the dipolar operator, $T_{\alpha\beta}$, is also expressed in terms of $\boldsymbol{r}_N$. For example

$$\langle 3d_{xz}|T_{zz}|3d_{xz}\rangle=N^2\int_0^\infty(3z_N{}^2/r_N{}^2-1)(x_N-X)^2\times(z_N-Z)^2\frac{e^{-2\beta r}}{r_N{}^3}dx_N\,dy_N\,dz_N \quad (27)$$

Then the homogenous polynomial is expanded in a series of products of the form

$$X^lY^mZ^nx^py^qz^r \quad (28)$$

where $(l+m+n+p+q+r)=6$ or 4 for dipolar integrals. Using equation (21) or (22), the product functions represented by equation (28) are transformed to products of spherical harmonics described by equation (23) and the radial part is also translated using equation (15).

Finally, the dipolar integral is then expressed in the following form

$$\langle\phi_{lm'}|T_{\alpha\beta}|\phi_{lm}\rangle=N^2\sum_{L_1,L_2}\sum_{M_1,M_2}\sum_{n=0}4\pi\int_0^\infty C_{m'm}(L_1,M_1;L_2,M_2)\,b_n(\boldsymbol{R},\boldsymbol{r}_N)\frac{d\,r_N}{r_N}\times\sum_{h=-n}^{n}Y_{nh}(\Theta,\Phi)\,Y_{L_1M_1}(\Theta,\Phi)\times\int_0^{2\pi}\int_0^\pi Y_{nh}(\theta_N,\phi_N)\,Y_{L_2M_2}(\theta_N,\phi_N)\sin\theta_N\,d\theta_N\,d\phi_N \quad (29)$$

Selection rules are obtained on n and h from equation (25). The evaluated dipolar integrals are listed in appendix.

(c) The Radial Integrals

To evaluate the hyperfine interaction integrals, the integrand is expressed as a function of $\boldsymbol{R}$ and $\boldsymbol{r}_N$ using equation (14) and (15). For the radial part of the integrals we introduce, for convenience, the following notation

$$r_n^{(L)}(t) = 4\beta^7(-R)^L \int_0^\infty r_N{}^{3-L}\, b_n(\boldsymbol{R}_1\boldsymbol{r}_N)\, d\boldsymbol{r}_N \tag{30}$$

and

$$\begin{aligned} u_n(t) &= r_n^{(4)}(t) \\ v_n(t) &= r_n^{(3)}(t) \\ w_n(t) &= r_n^{(2)}(t) \\ x_n(t) &= r_n^{(1)}(t) \\ y_n(t) &= r_n^{(0)}(t) \end{aligned} \tag{31}$$

where $t=2\beta R$. From the angular parts of hyperfine integrals, selection rules on n are obtained.
The required radial integrals are listed elsewhere[8,16].

3. Results

After evaluating a number of the dipolar integrals and the integrals of $l_{N\alpha}/r^3$ using the method in the previous section, a general expression is derived for the integrals

$\langle\phi_{lm'}|T_{\alpha\beta}|\phi_{lm}\rangle$ and $\langle\phi_{lm'}|l_{N\alpha}/r_N{}^3|\phi_{lm}\rangle$

by setting up in quite general terms the expression for the above integrals, and then extracting the coefficients of the various radial integrals. One example for 3d dipolar integrals is given

$$\begin{aligned} &\langle\phi_{2m'}|T_{\alpha\beta}|\phi_{2m}\rangle \\ &= C_6(5u_2+20v_3+30w_4+20x_5+5y_6)\,Y_{6q}(\Theta,\Phi) \\ &\quad C_4(5u_2+(20-A)v_1+Av_3+(30-B)w_2+Bw_4 \\ &\qquad +(20-C)x_3+Cx_5+5y_4)\,Y_{4q}(\Theta,\Phi) \\ &\quad C_2(5u_2+(20-A')v_1+A'v_3+(30-B'-C')w_0+B'w_2 \\ &\qquad +C'w_4+(20-A')x_1+A'x_3+5y_2)\,Y_{2q}(\Theta,\Phi) \\ &\quad C_0(5u_2+14v_1+6v_3+5/3(7w_0+11w_2) \\ &\qquad +20x_1+5y_0)\,Y_{0q}(\Theta,\Phi) \end{aligned} \tag{32}$$

In equation (32), the eleven unknowns q, A, B, C, A′, B′, C′, C_6, C_4, C_2 and C_0 are determined using a computer program which was written to calculate the large unmber of required matrix elements in an analytical form. Following Golding and Stubbs[8,20], the general formulas for each of the radial series for 3d orbitals are denoted as

$$\begin{aligned} F_j &= 5u_2+(20-A)v_1+Av_3+(30-B)w_2+Bw_4 \\ &\quad +(20-C)x_3+Cx_5+5y_4 \end{aligned} \tag{32a}$$

where

$$A=\mu,\quad B=10/7\mu-45/7,\quad C=5/9\mu-10/3$$

$$\begin{aligned} T_j &= 5u_2+(20-A)v_1+Av_3+(30-B-C)w_0+Bw_2 \\ &\quad +Cw_4+(20-A)x_1+Ax_3+5y_2 \end{aligned} \tag{32b}$$

where $A=\mu$, $B=10/3(\mu-\lambda+1)$, $C=\lambda$. The parameter values for the F_j and T_j series which we find are listed in Table 1.

The specific formulas for the integrals of $l_{N\alpha}/r^3$ whch we also find are

TABLE 1: Parameter Values for the F_j and T_j Series

F_j	F_{23}	F_{24}	F_{25}	F_{26}	F_{28}	F_{29}
μ	38/8	31	85/7	−2	324/25	6

T_j	T_{10}	T_{11}	T_{12}	T_{13}	T_{14}
μ	6	3	2	80/9	4
λ	15/7	6/7	3/7	92/21	9/7

$$\begin{aligned} t_3 &= y_2+1/5(14x_1+x_3)+1/3(7w_0+2w_2)+v_1 \\ t_4 &= y_2+1/10(21x_1+9x_3)+1/3(7w_0+2w_2)+v_1 \\ t_6 &= y_2+1/25(49x_1+26x_3)+1/15(14w_0+31w_2)+v_1 \\ t_7 &= y_2+1/5(-11x_1+22x_3)+1/3(-14w_0+23w_2)+v_1 \\ t_8 &= y_2+1/5(7x_1+8x_3)+3w_2+v_1 \end{aligned} \tag{32c}$$

When threefold axis is chosen as the quantization axis, the NMR shift arising from the electron orbital angular momentum and the electron spin dipolar–nuclear spin angular momentum interactions is given by

$$\Delta B/B = -\frac{\mu_0}{4\pi}\frac{\mu_B{}^2}{kT}\left\{\frac{d(\boldsymbol{R})+[1+\exp(3\zeta/2kT)]\,kT/\zeta\,S(R)}{1+2\exp(3\zeta/2kT)}\right\} \tag{33}$$

where

$$\begin{aligned} d(\boldsymbol{R}) &= -\frac{614400}{t^7}\sqrt{\frac{\pi}{26}}\left\{\frac{4\sqrt{2}}{9}\,Y_{60}(\Theta,\Phi)\right. \\ &\quad \pm\frac{1}{9}\sqrt{\frac{33}{3}}[Y_{6-3}(\Theta,\Phi)-Y_{63}(\theta,\Phi)] \\ &\quad \left.+\frac{1}{9}\sqrt{\frac{77}{6}}[Y_{6-6}(\theta,\Phi)+Y_{66}(\Theta,\Phi)]\right\}M(t) \\ &\quad -\frac{7168}{t^5}\sqrt{\frac{\pi}{21}}\left\{\frac{1}{3}\sqrt{\frac{7}{3}}\,Y_{40}(\Theta,\Phi)\right. \\ &\quad \left.\mp\frac{1}{3}\sqrt{\frac{10}{3}}[Y_{4-3}(\Theta,\Phi)-Y_{43}(\Theta,\Phi)]\right\}E(t) \\ &\quad +\frac{16\sqrt{\pi}}{105}\,J(t)\;Y_{00}(\Theta,\Phi) \\ S(\boldsymbol{R}) &= -\frac{614400}{t^7}\sqrt{\frac{\pi}{26}}\left\{\frac{4\sqrt{2}}{9}\,Y_{60}(\Theta,\Phi)\right. \\ &\quad \pm\frac{1}{9}\sqrt{\frac{35}{3}}\,[Y_{6-3}(\Theta,\Phi)-Y_{63}(\Theta,\Phi)] \\ &\quad \left.+\frac{1}{9}\sqrt{\frac{77}{6}}\,[Y_{6-6}(\Theta,\Phi)+Y_{66}(\Theta,\Phi)]\right\}M(t) \\ &\quad +\frac{7168}{t_5}\sqrt{\frac{\pi}{21}}\left\{\frac{1}{3}\sqrt{\frac{7}{3}}\,Y_{40}(\Theta,\Phi)\right. \\ &\quad \left.\mp\frac{1}{3}\sqrt{\frac{10}{3}}\,[Y_{4-3}(\Theta,\Phi)-Y_{43}(\Theta,\Phi)]\right\}G(t) \\ &\quad -\frac{16\sqrt{\pi}}{63}\,Y_{00}(\Theta,\Phi)\,P(t) \end{aligned}$$

$$M(t)=\beta^3\left[1-e^{-t}\sum_{n=0}^{11}\frac{t^n}{n!}\right]$$

$$E(t)=\beta^3\left[1-e^{-t}\frac{8}{11}\frac{t^9}{9!}+\sum_{n=0}^{8}\frac{t^n}{n!}\right]$$

$$J(t)=\beta^3e^{-t}\left(\frac{2}{9}\frac{t^4}{4!}+\frac{t^3}{3!}+\frac{t^2}{2!}+t+1\right)$$

$$G(t)=\beta^3e^{-t}\left(\frac{16}{33}\frac{t^9}{9!}\right)$$

$$P(t)=\beta^3e^{-t}\left(-\frac{4}{45}\frac{t^4}{4!}+\sum_{n=0}^{3}\frac{t^n}{n!}\right) \qquad \text{with } t=2\beta R$$

Since this expression for $\Delta B/B$ is applicable for all values of

R we may readily determine from equation (33) the case when R→0, namely,

$$\frac{\Delta B}{B} \longrightarrow \frac{8\beta^3}{315}\frac{\mu_B^2}{kT}\left\{\frac{3-5\{1-\exp(3\zeta/2kT)\,kT/\zeta\}}{1+2\exp(3\zeta/2kT)}\right\}\frac{\mu_0}{4\pi} \tag{34}$$

When R is large, the terms in equation (33) involving the polar coordinates of the NMR nucleus may be expressed in terms of $1/R^5$ and $1/R^7$, namely,

$$\begin{aligned} d(\boldsymbol{R}) = \frac{1}{R^7}\Big\{&\frac{7200}{\beta^4}\sqrt{\frac{\pi}{26}}\Big[\frac{4\sqrt{2}}{9}Y_{60}(\Theta,\Phi) \\ &\pm\frac{1}{9}\sqrt{\frac{35}{5}}[Y_{6-3}(\Theta,\Phi)-Y_{63}(\Theta,\Phi)] \\ &+\frac{1}{9}\sqrt{\frac{77}{6}}[Y_{6-6}(\Theta,\Phi)+Y_{66}(\Theta,\Phi)]\Big\} \\ &+\frac{1}{R_5}\Big\{\frac{224}{\beta_4}\sqrt{\frac{\pi}{21}}\Big[\frac{1}{3}\sqrt{\frac{7}{3}}Y_{40}(\Theta,\Phi) \\ &\pm\frac{1}{3}\sqrt{\frac{10}{3}}Y_{4-3}(\Theta,\Phi)-Y_{43}(\Theta,\Phi)]\Big\} \\ S(\boldsymbol{R}) = \frac{1}{R^7}\Big\{&\frac{4800}{\beta^4}\sqrt{\frac{\pi}{26}}\Big[\frac{4\sqrt{2}}{9}Y_{60}(\Theta,\Phi) \\ &\pm\frac{1}{9}\sqrt{\frac{35}{3}}[Y_{6-3}(\Theta,\Phi)-Y_{63}(\Theta,\Phi)] \\ &+\frac{1}{9}\sqrt{\frac{77}{6}}Y_{6-6}(\Theta,\Phi)+Y_{66}(\Theta,\Phi)]\Big\} \end{aligned} \tag{35}$$

4. Discussion

We find from equation (32a–32c) that the radial series for dipolar integrals and the integrals of $l_{Na}/r_N{}^3$ follow 1:4:6:4:1 and 1:3:3:1 patterns, respectively. This is agreement with the previous reports[16].

The calculated NMR shifts along the x, y and z axis using equation (33) for a $3d^1$ system in a strong octahedral crystal field are listed in Table 2(a) when we choose the threefold axis to be our axis of quantization, and in Table 2(b) when the z axis is chosen as the quantization axis, respectively. Here we choose $\beta=4/3a_0$, the spin-orbit coupling constant as 154 cm^{-1}. These parameter values are similar to those of Ti^{3+} ion. The temperature is taken as T=300 K. The isoshielding diagram is represented in Figure 2 when the threefold axis is chosen to be our axis of quantization.

The NMR results along the <100>, <110> and <111> axes for a $3d^1$ system in a strong octahedral crystal field are also listed in Table 3(a) when the threefold axis is chosen as the quantization axis and in Table 3(b) when the z axis is chosen to be our axis of quantization. When we choose the threefold axis to be the quantization axis, the NMR shift, $\Delta B/B$, decreases in magnitude rapidly as R increases. Along the <100> and <010> axes, $\Delta B/B$ is positive for all values of R, while along the <001> axis, $\Delta B/B$ changes sign when R=0.10 nm. However, the NMR shift, $\Delta B/B$, is negative for all values of R along the <100>, <010> and <001> axes when the z axis is chosen as the quantization axis. It is found that along the <110> axis, $\Delta B/B$ is positive for all values of R while along <111> axis, $\Delta B/B$ is negative when the threefold axis is chosen as the quantization axis. However, when the z axis is chosen to be the quantization

TABLE 2 (a): $\Delta B/B$(ppm) for Specific R-Values for a $3d^1$ System in a Strong Crystal Environment of Octahedral Symmetry When the Threefold Axis is Chosen as the Quantization Axis

R(nm)	$\Delta B/B$(ppm)		
	<100> axis	<010> axis	<001> axis
0.05	99662.961	154187.581	−290428.751
0.1	831.121	1259.553	−1327.738
0.15	50.810	77.804	40.701
0.2	23.394	27.761	48.170
0.25	11.755	12.785	24.277
0.3	5.468	5.823	11.517
0.35	2.624	2.742	5.726
0.4	1.338	1.390	3.049
0.45	0.736	0.759	1.731
0.50	0.431	0.442	1.039

TABLE 2(b): $\Delta B/B$(ppm) for Specific R-Values for a $3d^1$ System in a Strong Crystal Environment of Octahedral Symmetry When the z Axis is Chosen as the Quantization Axis

R(nm)	$\Delta B/B$(ppm)		
	<100> axis	<010> axis	<001> axis
0.05	−783171.948	−783171.948	−783171.948
0.1	−8824.801	−8824.801	−8824.801
0.15	−935.306	−935.306	−935.306
0.2	−215.365	−215.365	−215.365
0.25	−67.986	−67.986	−67.986
0.3	−26.049	−26.049	−26.049
0.35	−11.549	−11.549	−11.549
0.4	−5.732	−5.732	−5.732
0.45	−3.105	−3.105	−3.105
0.5	−1.801	−1.801	−1.801

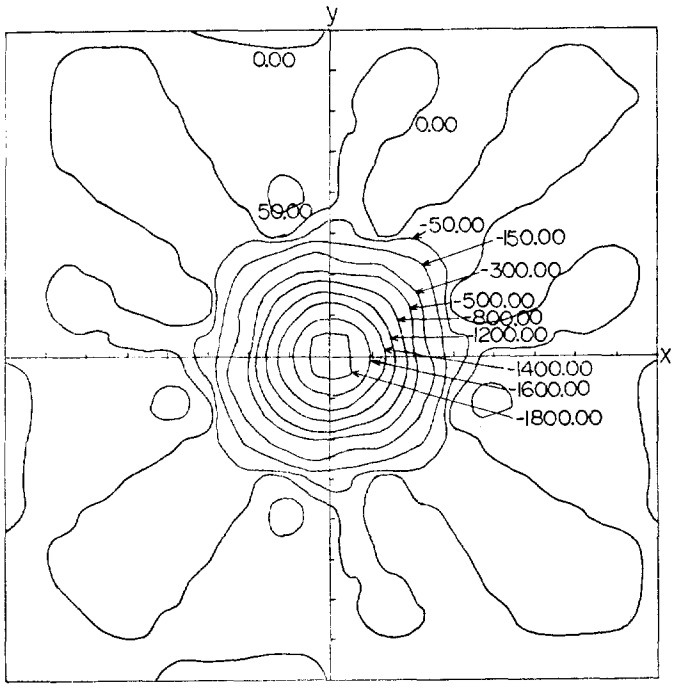

Figure 2. Isoshielding diagram in xy plane for $3d^1$ system when the threefold axis is chosen as the quantization axis. Here we choose the temperature as T=300 K, the spin–orbit coupling constant as 154 cm^{-1} and $\beta=4/3a_0$.

TABLE 3(a): $\Delta B/B$(ppm) for Specific R-values for a $3d^1$ System in a Strong Crystal Field of Octahedral Symmetry When the Threefold Axis is Chosen as the Quantization Axis

R(nm)	$\Delta B/B$(ppm)		
	⟨100⟩ axis	⟨010⟩ axis	⟨001⟩ axis
0.05	99662.961	126925.271	−84591.999
0.1	831.121	1045.337	−1531.827
0.15	50.810	64.307	−225.207
0.2	23.394	25.578	−47.926
0.25	11.755	12.315	−12.765
0.3	5.468	5.645	−4.405
0.35	2.614	2.678	−1.888
0.40	1.338	1.364	−0.935
0.45	0.736	0,748	−0.510
0.50	0.431	0.447	−0.297

TABLE 3(b): $\Delta B/B$(ppm) for Specific R-values for a $3d^1$ System in a Strong Crystal Field of Octahedral Symmetry When the z Axis is Chosen to be Our Axis of Quantization

R(nm)	$\Delta B/B$(ppm)		
	⟨100⟩ axis	⟨010⟩ axis	⟨001⟩ axis
0.05	−783171.948	1154326.66	−1187769.763
0.1	−8824.801	9118.237	−8378.677
0.15	−935.306	572.948	−403.550
0.2	−215.365	107.863	−23.698
0.25	−67.986	33.420	5.844
0.3	−26.049	12.335	5.673
0.35	−11.549	5.092	3.617
0.4	−5.732	2.334	2.202
0.45	−3.105	1.176	1.357
0.5	−1.801	0.642	0.859

axis, $\Delta B/B$ along the $\langle 110\rangle$ axis is positive for all values of R while along the $\langle 111\rangle$ axis, $\Delta B/B$ changes sign when R = 0.20 nm, the values being negative for smaller R values and positive for greater R values. It is interesting to note that when the threefold axis is chosen to be our axis of quantization, the $\Delta B/B$ values along the $\langle 100\rangle$, $\langle 010\rangle$ and $\langle 001\rangle$ axes are different from each other for all values of R, while those along the $\langle 100\rangle$, $\langle 010\rangle$ and $\langle 001\rangle$ axes are exactly the same when the z axis is chosen as the quantization axis.

The NMR results for a $3d^1$ system using equation (33) and the corresponding multipolar terms, $1/R^5$ and $1/R^7$, given by equation (35) are shown in Table 4 (a-c), 5(a) and 6(a) when the threefold axis is chosen as the quantization axis and in Table 4(d), 5(b) and 6(b) when the z axis is chosen to be our axis of quantization.

A comparison of the multipolar terms with the exact solution given by equation (33) shows that $1/R^7$ term(octapolar term) contributes dominantly to the NMR shift for all values of R. However, the $1/R^7$ term is inadequate to describe accurately the NMR shift for R<0.50 nm. When the $1/R^5$ term is included, there is good agreement when R=0.35 nm. It is found that along the $\langle 001\rangle$ axis, $1/R^5$ term gives values opposite in sign to that of $1/R^7$ term when the threefold axis

TABLE 4: A Comparison of the Exact value of $\Delta B/B$(ppm) using Equation(33) with the Multipolar Terms for Specific R-Values

(a) Along the ⟨200⟩ axis

R(nm)	$\Delta B/B$(ppm)			
	$1/R^5$	$1/R^7$	sum of all multipolar terms	From eq. (33)
0.05	80361.389	20799.309	101160.697	99662.961
0.1	631.447	707.226	1338.673	831.121
0.15	39.785	120.107	159.892	50.810
0.2	6.436	35.277	41.713	23.394
0.25	1.651	12.748	14.430	11.755
0.3	0.523	5.289	5.812	5.468
0.35	0.189	2.466	2.655	2.614
0.4	0.076	1.267	1.343	1.338
0.45	0.034	0.703	0.737	0.736
0.5	0.016	0.415	0.431	0.431

(b) Along th ⟨010⟩ axis

R(nm)	$\Delta B/B$(ppm)			
	$1/R^5$	$1/R^7$	sum of all multipolar terms	From eq. (33)
0.05	134886.009	20799.309	155685.318	154187.581
0.1	1059.879	707.226	1767.105	1259.553
0.15	66.779	120.107	186.885	77.804
0.2	10.803	35.277	46.080	27.761
0.25	2.770	12.748	15.519	12.875
0.3	0.878	5.289	6.167	5.823
0.35	0.317	2.466	2.784	2.742
0.4	0.127	1.267	1.394	1.390
0.45	0.056	0.703	0.760	0.759
0.5	0.027	0.415	0.442	0.442

(c) Along the ⟨001⟩ axis

R(nm)	$\Delta B/B$(ppm)			
	$1/R^5$	$1/R^7$	sum of all multipolar terms	From eq. (33)
0.05	−344395.837	55464.823	−288931.014	−290428.751
0.1	−2706.122	1885.935	−820.186	−1327.738
0.15	−270.502	320.284	149.782	40.701
0.2	−27.583	94.071	66.488	48.170
0.25	−7.075	33.996	26.921	24.277
0.3	−2.243	14.104	11.861	11.517
0.35	−0.809	6.577	5.768	5.726
0.4	−0.325	3.379	3.054	3.049
0.45	−0.144	1.875	1.732	1.731
0.5	−0.069	1.107	1.034	1.039

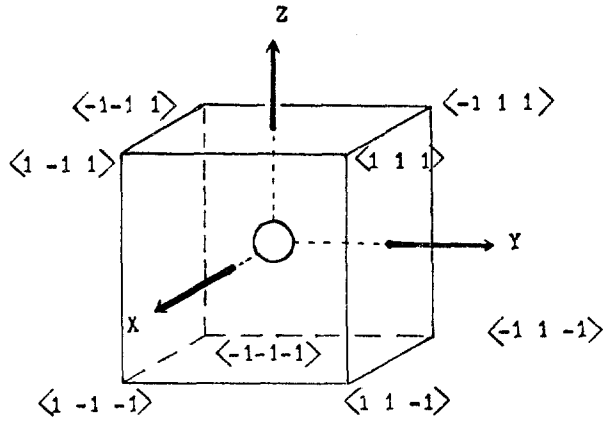

Figure 3. Coordinate System of the octahedron.

(d) A Comparison of the Exact Value of $\Delta B/B$(ppm) Using eq. (12) of Reference (8) with the Multipolar Terms for Specific R-Values Along the ⟨100⟩, ⟨010⟩ and ⟨001⟩ Axis

R(nm)	$\Delta B/B$(ppm)			
	$1/R^5$	$1/R^7$	sum of all multipolar terms	exat
0.05	−698476.978	−83197.234	−781674.212	−783171.958
0.1	−5488.346	−2828.903	−8317.249	−8824.301
0.15	−345.799	−480.427	−826.225	−935.306
0.2	−55.941	−141.106	−197.047	−215.365
0.25	−14.348	−50.994	−65.342	−67.986
0.3	−4.548	−21.156	−25.705	−26.049
0.35	−1.642	−9.866	−11.508	−11.549
0.4	−0.660	−5.068	−5.728	−5.723
0.45	−0.291	−2.813	−3.104	−3.105
0.5	−0.140	−1.661	−1.801	−1.801

TABLE 5(a): A Comparison of the Exact value of $\Delta B/B$(ppm) Using eq. (33) with the Multipolar Terms for Specific R-Values Along the ⟨110⟩ Axis When the Threefold Axis is Chosen as the Quantization Axis

R(nm)	$\Delta B/B$(ppm)			
	$1/R^5$	$1/R^7$	sum of all multipolar terms	from eq. (33)
0.05	107623.699	20799.309	128423.008	126935.271
0.1	845.663	707.226	1552.889	1045.337
0.25	53.282	120.107	173.388	64.307
0.2	8.620	35.277	43.896	25.578
0.25	2.211	12.748	14.959	12.315
0.3	0.701	5.289	5.990	5.645
0.35	0.253	2.466	2.719	2.678
0.4	0.102	1.267	1.369	1.364
0.45	0.045	0.703	0.748	0.748
0.5	0.022	0.415	0.437	0.437

TABLE 5(b): A Comparison of the Exact Value of $\Delta B/B$(ppm) using eq. (12) Reference (8) with the Multipolar Terms for Specific R-Vnlues Along the ⟨110⟩ Axis When We Choose the z Axis to be Our Axis of Quantization

R(nm)	$\Delta B/B$(ppm)			
	$1/R^5$	$1/R^7$	sum of all multipolar terms	exact
0.05	1135025.088	20799.309	1155824.397	1154326.66
0.1	8914.563	707.226	9625.789	9118.237
0.15	561.923	120.107	682.029	572.948
0.2	90.904	35.277	126.181	107.863
0.25	23.316	12.749	36.064	33.420
0.3	7.391	5.289	12.681	12.335
0.35	2.668	2.466	5.134	5.092
0.4	1.072	1.267	2.339	2.334
0.45	0.473	0.703	1.177	1.176
0.5	0.227	0.415	0.642	0.642

is chosen as the quantization axis while along the ⟨111⟩ axis, the same holds true when the z axis is chosen to be our axis of quantization. $\sin\Theta_i$, $\cos\Theta_i$ and $\cos(3\Phi_i)$ are listed in Table 7 when we choose the various values of Θ_i and Φ_i corresponding to ⟨111⟩, ⟨-1-1-1⟩, ⟨-11-1⟩, ⟨1-11⟩, ⟨-1-11⟩, ⟨11-1⟩ ⟨1-1-1⟩ and ⟨-111⟩ axes represented in Figure 3. Since the linear combimation of spherical

TABLE 6(a): A Comparison of the Exact Value of $\Delta B/B$(ppm) Using Equation (33) with the Multipolar Terms for Specific R-Values Along the ⟨111⟩ Axis When the Threefold axis is Chosen as the Qiantization axis

R(nm)	$\Delta B/B$(ppm)			
	$1/R^5$	$1/R^7$	sum of all multipolar terms	from eq. (33)
0.05	−68890.505	−14203.757	−83094.262	−84591.999
0.1	−541.313	−482.961	−1024.275	−1531.827
0.25	−34.106	−82.020	−116.126	−225.207
0.2	−5.517	−24.090	−29.608	−47.926
0.25	−1.415	−8.706	−10.121	−12.765
0.3	−0.449	−3.612	−4.060	−4.505
0.35	−0.612	−1.684	−1.846	−1.888
0.4	−0.065	−0.865	−0.930	−0.935
0.45	−0.029	−0.480	−0.609	−0.510
0.5	−0.014	−0.284	−0.297	−0.297

TABLE 6(b): A Comparison of the Exact value of $\Delta B/B$(ppm) using Equation (33) with the Multipolar Terms for Specific R-Values Along the ⟨111⟩ Axis When the z Axis is Chosen as the Quantization Axis

R(nm)	$\Delta B/B$(ppm)			
	$1/R^5$	$1/R^7$	sum of all multipolar terms	from eq. (33)
0.05	−1241736.849	55464.823	−1186272.026	−84591.999
0.1	−9757.060	1885.935	−7871.125	−1531.827
0.15	−614.753	320.284	−294.469	−225.207
0.2	−99.451	94.071	−7.380	−47.926
0.25	−25.508	33.996	8.488	−12.765
0.3	−8.086	14.104	6.018	−4.405
0.35	−2.918	6.577	3.658	−1.888
0.4	−1.172	3.379	2.206	−0.935
0.45	−0.518	1.875	1.358	−0.510
0.5	−0.518	1.875	1.358	−0.510
0.5	−0.248	1.107	0.859	−0.297

harmonics, $(Y_{4-3}-Y_{43})$ and $(Y_{6-3}-Y_{63})$, can be expressed by a linear combination of the products of $\sin\Theta_i$, $\cos\Theta_i$ and $\cos(3\Phi_i)$ as

$$(Y_{4-3}-Y_{43})=\frac{3}{4}\sqrt{\frac{35}{\pi}}\sin^3\Theta_i\cos\Theta_i\cos(3\Phi_i)$$

$$(Y_{6-3}-Y_{63})=\frac{3}{4}\sqrt{\frac{1365}{\pi}}\sin^3\Theta_i(11\cos^3\Theta_i-3\cos\Theta_i)\times\cos(3\Phi_i) \quad (36)$$

The sign of $(Y_{4-3}-Y_{43})$ and $(Y_{6-3}-Y_{63})$ are determined by those of $\cos(3\Phi_i)$, $\sin\Theta_i$ and $\cos\Theta_i$. As shown in Table 7, the sign of products of $\cos(3\Phi_i)$, $\sin\Theta_i$ and $\cos\Theta_i$ along the ⟨111⟩, ⟨-1-1-1⟩, ⟨-11-1⟩ and ⟨1-11⟩ axes are opposite to those along the ⟨-1-11⟩, ⟨11-1⟩, ⟨1-1-1⟩ and ⟨-111⟩ axes when we express the sine and cosine functions in terms of the smallest angles. The sign of $(Y_{4-3}-Y_{43})$ and $(Y_{6-3}-Y_{63})$ along the ⟨111⟩, ⟨-1-11⟩, ⟨-11-1⟩ and ⟨1-11⟩ axes are therefore opposite to those along the ⟨-1-11⟩, ⟨11-1⟩, ⟨1-1-1⟩ and ⟨-111⟩ exes. The magnitude of $(Y_{4-3}-Y_{43})$ and $(Y_{6-3}-Y_{63})$ along the above axes is, however, the same. By operating upon the linear combination of spherical harmonics, $(Y_{4-3}-Y_{43})$ and and $(Y_{6-3}-Y_{63})$ with C_2, we have

TABLE 7: The Signs of Spherical Harmonics, $[Y_{4-3}-Y_{43}]$ and $[Y_{6-3}-Y_{63}]$, When We Choose the Various Values of Θ_i and Φ_i Listed

axis	Θ_i	Φ_i	$3\Phi_i$	$\cos(3\Phi_i)$	$\sin\Theta_i$	$\cos\Theta_i$	sign of spherical harmonics	
							$(Y_{4-3}-Y_{43})$	$(Y_{6-3}-Y_{63})$
⟨111⟩	54.74	45	136	$-\cos 45$	sin 54.74	cos 54.74	−	−
⟨-1-1-1⟩	125.26	225	675	cos 45	sin 54.75	$-\cos 54.74$	−	−
⟨-11-1⟩	125.26	135	405	cos 45	sin 54.74	$-\cos 54.74$	−	−
⟨1-11⟩	54.74	315	945	cos 45	sin 54.74	cos 54.74	−	−
⟨-1-11⟩	54.74	225	676	cos 45	sin 54.74	cos 54.74	+	+
⟨11-1⟩	125.26	45	135	$-\cos 45$	sin 54.74	$-\cos 54.74$	+	+
⟨1-1-1⟩	125.26	316	945	$-\cos 45$	sin 54.74	$-\cos 54.74$	+	+
⟨-111⟩	54.74	135	405	cos 45	sin 54.74	cos 54.74	+	+

$$C_2(Y_{4-3}-Y_{43}) = -(Y_{4-3}-Y_{43})$$
$$C_2(Y_{6-3}-Y_{63}) = -(Y_{6-3}-Y_{63}) \quad (37)$$

This symmetry operation corresponds to a rotation of 180 degree counterclockwisely about z axis. In order for the trace under C_2 to be 1, the sign along the⟨111⟩ axis must be equal to that along the ⟨-1-11⟩, This means that the sign of the linear combination of spherical harmonics, $(Y_{4-3}-Y_{43})$ and $(Y_{6-3}-Y_{63})$, changes in third quadrant. We observe further that $C_2'(Y_{4-3}-Y_{43})=(Y_{4-3}-Y_{43})$ and $C'_2(Y_{6-3}-Y_{63})=(Y_{6-3}-Y_{63})$. This symmetry operation corresponds to a rotation of 180 degree about y axis. The sign of $(Y_{4-3}-Y_{43})$ and $(Y_{6-3}-Y_{63})$ along the ⟨111⟩ axis is the same as that along ⟨-11-1⟩. Since a rotation of 180 degree about x axis transforms the ⟨111⟩ axis to ⟨-1-1-1⟩ axis, we can easily find that $C_2''(Y_{4-3}-Y_{43})=(Y_{4-3}-Y_{43})$ and $C_2''(Y_{6-3}-Y_{63})=(Y_{6-3}-Y_{63})$. Such arguments indicate that along the ⟨111⟩ axis the sgins of $(Y_{6-3}-Y_{63})$ and $(Y_{4-3}-Y_{43})$ must be equal to those along the ⟨-11-1⟩, ⟨-1-1-1⟩ and ⟨1-11⟩ axes but opposite to those along the ⟨-1-11⟩, ⟨11-1⟩, ⟨1-1-1⟩ and ⟨-111⟩ axes. We see further that the sign of $(Y_{4-3}-Y_{43})$ and $(Y_{6-3}-Y_{63})$ in first and third quadrants is opposite to that in second and fourth quadrants.

It is interesting to note that along the ⟨111⟩, ⟨-1-1-1⟩, ⟨-11-1⟩, ⟨1-11⟩, ⟨-1-11⟩, ⟨11-1⟩, ⟨1-1-1⟩ and ⟨-111⟩ axes, $\Delta B/B$ is exactly the same when the threefold axis is chosen as the quantization axis. The same holds true when the z axis is chosen to be our axis of quantization.

This work can be applied to determine the NMR shift for $3d^n$ systems and the hyperfine tensor components in a strong crystal field of octahedral and trigonal symmetries when the threefold axis is chosen as the quantization axis. No theoretical calculation of $\Delta B/B$ for $3d^1$ system in a strong crystal field of octahedral symmetry has been carried out when the threefold axis is chosen as the quantization axis and no experimental NMR shift has been reported.

Appendix : the Hyperfine Integrals

(a) The integrals of $\hat{l}_{N\alpha}/r_N^3$

$$i\langle d_{z^2}|\hat{l}_{Nz}/r^3|d_{x^2-y^2}\rangle$$
$$=\frac{4}{21}\sqrt{\frac{2\pi}{45}}[Y_{2-2}(\Theta,\Phi)-Y_{22}(\Theta,\Phi)]t_3$$
$$-\frac{4}{41}\sqrt{\frac{\pi}{30}}[Y_{4-2}(\Theta,\Phi)-Y_{42}(\Theta,\Phi)]f_1$$
$$i\langle d_{xy}|\hat{l}_{Nz}/r_N^3|d_{z^2}\rangle$$
$$=\frac{4}{63}\sqrt{\frac{2\pi}{5}}[Y_{2-2}(\Theta,\Phi)+Y_{22}(\Theta,\Phi)]t_3-\frac{4}{63}\sqrt{\frac{3\pi}{10}}$$
$$[Y_{4-2}(\Theta,\Phi)-Y_{42}(\Theta,\Phi)]f_1$$
$$i\langle d_{xz}|\hat{l}_{Nz}/r_N^3|d_{z^2}\rangle$$
$$=\frac{1}{21}\sqrt{\frac{2\pi}{45}}Y_{2-1}(\Theta,\Phi)+Y_{21}(\Theta,\Phi)]t_7+\frac{2}{21}\sqrt{\frac{\pi}{15}}$$
$$[Y_{4-1}(\Theta,\Phi)+Y_{41}(\Theta,\Phi)]f_1$$
$$i\langle d_{yz}|\hat{l}_{Nz}/r_N^3|d_{z^2}\rangle$$
$$=-\frac{1}{63}\sqrt{\frac{2\pi}{5}}[Y_{2-1}(\Theta,\Phi)+Y_{21}(\Theta,\Phi)]t_7-\frac{2}{21}\sqrt{\frac{\pi}{15}}$$
$$[Y_{4-1}(\Theta,\Phi)-Y(\Theta,\Phi)]f_1$$
$$i\langle d_{xy}|_N\hat{l}_{Nz}/r_N^3|d_{x^2-y^2}\rangle$$
$$=-\frac{8\sqrt{\pi}}{45}Y_{00}(\Theta,\Phi)n_1+\frac{16}{63}\sqrt{\frac{\pi}{5}}Y_{20}(\Theta,\Phi)t_4-\frac{8\sqrt{\pi}}{315}$$
$$Y_{40}(\Theta,\Phi)f_1$$
$$i\langle d_{yz}|\hat{l}_{Nz}/r_N^3|d_{x^2-y^2}\rangle$$
$$=-\frac{1}{7}\sqrt{\frac{2\pi}{15}}[Y_{2-1}(\Theta,\Phi)-Y_{21}(\Theta,\Phi)]t_2+\frac{1}{21}\sqrt{\frac{\pi}{5}}$$
$$[Y_{4-1}(\Theta,\Phi)-Y_{41}(\Theta,\Phi)]f_1$$
$$+\frac{1}{9}\sqrt{\frac{\pi}{35}}[Y_{4-3}(\Theta,\Phi)-Y_{43}(\Theta,\Phi)]f_1$$
$$i\langle d_{z^2}|\hat{l}_{Nx}/r_N^3|d_{x^2-y^2}\rangle$$
$$=\frac{4}{63}\sqrt{\frac{2\pi}{5}}[Y_{2-1}(\Theta,\Phi)+Y_{21}(\Theta,\Phi)]t_3+\frac{1}{21}\sqrt{\frac{\pi}{15}}$$
$$[Y_{4-1}(\Theta,\Phi)+Y_{41}(\Theta,\Phi)]f_1$$
$$-\frac{1}{3}\sqrt{\frac{\pi}{105}}[Y_{4-3}(\Theta,\Phi)+Y_{43}(\Theta,\Phi)]f_1$$
$$i\langle d_{xy}|_{Nx}/r_N^3|d_{z^2}\rangle$$
$$=\frac{4}{63}\sqrt{\frac{2\pi}{5}}[Y_{2-1}(\Theta,\Phi)-Y_{21}(\Theta,\Phi)]t_3+\frac{1}{21}\sqrt{\frac{\pi}{15}}$$
$$[Y_{4-1}(\Theta,\Phi)-Y_{41}(\Theta,\Phi)]f_1$$
$$-\frac{1}{9}\sqrt{\frac{\pi}{15}}[Y_{4-3}(\Theta,\Phi)-Y_{43}(\Theta,\Phi)]f_1$$
$$i\langle d_{xz}|\hat{l}_{Nx}/r_N^3|d_{z^2}\rangle$$
$$=\frac{5}{63}\sqrt{\frac{2\pi}{5}}[Y_{2-2}(\Theta,\Phi)-Y_{22}(\Theta,\Phi)]t^9+\frac{1}{21}\sqrt{\frac{2\pi}{15}}$$
$$[Y_{4-2}(\Theta,\Phi)-Y_{42}(\Theta,\Phi)]f_1$$
$$i\langle d_{yz}|\hat{l}_{Nx}/r_N^3|d_{z^2}\rangle$$
$$=\frac{4\sqrt{3\pi}}{45}Y_{00}(\Theta,\Phi)+\frac{2}{7}\sqrt{\frac{\pi}{15}}Y_{20}(\Theta,\Phi)t_2-\frac{5}{63}\sqrt{\frac{2\pi}{5}}$$
$$[Y_{2-2}(\Theta,\Phi)+Y_{22}(\Theta,\Phi)]t_6+\frac{4}{105}\sqrt{\frac{\pi}{3}}$$
$$Y_{40}(\Theta,\Phi)f_1-\frac{2}{63}\sqrt{\frac{3\pi}{10}}$$
$$[Y_{4-2}(\Theta,\Phi)+Y_{42}(\Theta,\Phi)]f_1$$
$$i\langle d_{xy}|\hat{l}_{Nx}/r_N^3|d_{x^2-y^2}\rangle$$

$$=\frac{2}{63}\sqrt{\frac{2\pi}{5}}[Y_{2-1}(\Theta,\Phi)-Y_{21}(\Theta,\Phi)]\,t_8-\frac{2}{63}\sqrt{\frac{\pi}{15}}$$
$$[Y_{4-1}(\Theta,\Phi)-Y_{41}(\Theta,\Phi)]\,f_1$$
$$i\langle d_{yz}|\hat{l}_{Nx}/r_N{}^3|d_{x^2-y^2}\rangle$$
$$=\frac{4\sqrt{\pi}}{45}Y_{00}(\theta,\Phi)\,n_1-\frac{2}{63}\sqrt{\frac{\pi}{5}}Y_{20}(\theta,\Phi)\,t_1-\frac{1}{7}\sqrt{\frac{2\pi}{15}}$$
$$[Y_{2-2}(\Theta,\Phi)+Y_{22}(\Theta,\Phi)]t_2-\frac{2\sqrt{\pi}}{105}$$
$$Y_{42}[\Theta,\Phi]\,f_1+\frac{2}{63}\sqrt{\frac{\pi}{10}}$$
$$[Y_{4-2}(\Theta,\Phi)+Y_{42}(\Theta,\Phi)]\,f_1+\frac{1}{9}\sqrt{\frac{2\pi}{35}}$$
$$[Y_{4-4}(\Theta,\Phi)+Y_{41}(\Theta,\Phi)]\,f_1$$
$$i\langle d_{xz}|\hat{l}_{Nx}/r_N{}^3|d_{x^2-y^2}\rangle$$
$$=\frac{1}{63}\sqrt{\frac{2\pi}{5}}[Y_{2-2}(\Theta,\Phi)-Y_{22}(\Theta,\Phi)]\,t_1+\frac{2}{63}\sqrt{\frac{2\pi}{15}}$$
$$[Y_{4-2}(\Theta,\Phi)-Y_{42}(\Theta,\Phi)]\,f_1-\frac{1}{9}\sqrt{\frac{2\pi}{105}}$$
$$[Y_{4-4}(\Theta,\Phi)-Y_{44}(\Theta,\Phi)]\,f_1$$
$$i\langle d_{z^2}|\hat{l}_{Ny}/r_N{}^3|d_{x^2-y^2}\rangle$$
$$=\frac{4}{63}\sqrt{\frac{2\pi}{5}}[Y_{2-1}(\Theta,\Phi)-Y_{21}(\Theta,\Phi)]\,t_3+\frac{1}{21}\sqrt{\frac{\pi}{15}}$$
$$[Y_{4-1}(\Theta,\Phi)-Y_{41}(\Theta,\Phi)]\,f_1$$
$$+\frac{1}{9}\sqrt{\frac{\pi}{15}}[Y_{4-3}(\Theta,\Phi)-Y_{43}(\Theta,\Phi)]\,f_1$$
$$i\langle d_{xy}|\hat{l}_{Ny}/r_N{}^3|d_{z^2}\rangle$$
$$=-\frac{4}{63}\sqrt{\frac{2\pi}{5}}[Y_{2-1}(\Theta,\Phi)+Y_{21}(\Theta,\Phi)]\,t_3-\frac{1}{21}\sqrt{\frac{\pi}{15}}$$
$$[Y_{4-1}(\Theta,\Phi)+Y_{41}(\Theta,\Phi)]\,f_1$$
$$-\frac{1}{3}\sqrt{\frac{\pi}{105}}[Y_{4-3}(\Theta,\Phi)+Y_{43}(\Theta,\Phi)]\,f_1$$
$$i\langle d_{xz}|l_{Ny}/r_N{}^3|d_{z^2}\rangle$$
$$=-\frac{4\sqrt{3\pi}}{45}Y_{00}(\Theta,\Phi)\,n_1-\frac{2}{7}\sqrt{\frac{\pi}{15}}Y_{20}(\Theta,\Phi)\,t_2-\frac{5}{63}\sqrt{\frac{2\pi}{5}}$$
$$[Y_{2-2}(\Theta,\Phi)+Y_{22}(\Theta,\Phi)]\,t_6$$
$$-\frac{4}{105}\sqrt{\frac{\pi}{3}}Y_{40}(\Theta,\Phi)\,f_1-\frac{2}{63}\sqrt{\frac{3\pi}{10}}$$
$$[Y_{4-2}(\Theta,\Phi)+Y_{42}(\Theta,\Phi)]\,f_1$$
$$i\langle d_{yz}|\hat{l}_{Ny}/r_N{}^3|d_{z^2}\rangle$$
$$=-\frac{5}{63}\sqrt{\frac{2\pi}{5}}[Y_{2-2}(\Theta,\Phi)-Y_{22}(\Theta,\Phi)\,t_6-\frac{1}{21}\sqrt{\frac{2\pi}{15}}$$
$$[Y_{4-2}(\Theta,\Phi)-Y_{42}(\Theta,\Phi)]\,f_1$$
$$i\langle d_{xy}|\hat{l}_{Ny}/r_N{}^3|d_{x^2-y^2}\rangle$$
$$=\frac{2}{21}\sqrt{\frac{2\pi}{15}}[Y_{2-1}(\Theta,\Phi)+Y_{21}(\Theta,\Phi)]\,t_8-\frac{2}{63}\sqrt{\frac{\pi}{5}}$$
$$[Y_{4-1}(\Theta,\Phi)+Y_{41}(\Theta,\Phi)]\,f_1$$
$$i\langle d_{yz}|\hat{l}_{NY}/r_N{}^3|d_{x^2-y^2}\rangle$$
$$=\frac{2}{21}\sqrt{\frac{2\pi}{15}}[Y_{2-2}(\Theta,\Phi)-Y_{22}(\Theta,\Phi)]\,t_1+\frac{2}{63}\sqrt{\frac{2\pi}{5}}$$
$$[Y_{4-2}(\Theta,\Phi)-Y_{42}(\Theta,\Phi)]\,f_1$$
$$+\frac{1}{9}\sqrt{\frac{2\pi}{35}}[Y_{4-4}(\Theta,\Phi)-Y_{44}(\Theta,\Phi)]\,f_1$$

(b) The Dipolar Integrals

$$\langle d_{x^2-y^2}|T_{zx}|d_{z^2}\rangle$$
$$=\frac{4}{105}\sqrt{\frac{2\pi}{5}}[Y_{2-1}(\Theta,\Phi)-Y_{21}(\Theta,\Phi)]T_4+\frac{2}{165}\sqrt{\frac{\pi}{15}}$$
$$[Y_{4-1}(\theta,\Theta)-Y_{41}(\Theta,\Phi)]\,F_{25}$$
$$-\frac{2}{165}\sqrt{\frac{\pi}{105}}[Y_{4-3}(\Theta,\Phi)-Y_{43}(\Theta,\Phi)]F_{24}-\frac{2}{165}\sqrt{\frac{2\pi}{91}}$$
$$[Y_{6-1}(\Theta,\Phi)-Y_{61}(\Theta,\Phi)]\,S_1$$
$$+\frac{4}{55}\sqrt{\frac{\pi}{455}}[Y_{6-3}(\Theta,\Phi)-Y_{63}(\Theta,\Phi)]\,S_1$$
$$\langle d_{xz}|T_{zx}|d_{z^2}\rangle$$
$$=\frac{4}{525}\sqrt{\frac{\pi}{3}}Y_{00}(\Theta,\Phi)\,N_1+\frac{4}{105}\sqrt{\frac{\pi}{15}}Y_{20}(\Theta,\Phi)\,T_{11}$$
$$-\frac{2}{105}\sqrt{\frac{2\pi}{5}}[Y_{2-2}(\Theta,\Phi)+Y_{22}(\Theta,\Phi)]\,T_4$$
$$-\frac{8}{5775}\sqrt{\frac{\pi}{3}}Y_{40}(\Theta,\Phi)\,F_{24}+\frac{4}{165}\sqrt{\frac{\pi}{30}}[Y_{4-2}(\Theta,\Phi)$$
$$+Y_{42}(\Theta,\Phi)]\,F_{25}-\frac{16}{385}\sqrt{\frac{\pi}{39}}Y_{60}(\Theta,\Phi)S_1+\frac{16}{165}\sqrt{\frac{\pi}{455}}$$
$$[Y_{6-2}(\Theta,\Phi)+Y_{62}(\Theta,\Phi)]\,S_1$$
$$\langle d_{x^2-y^2}|T_{xx}|d_{x^2-y^2}\rangle$$
$$=\frac{8\sqrt{\pi}}{1375}Y_{00}(\Theta,\Phi)\,N_1-\frac{4}{315}\sqrt{\frac{\pi}{5}}Y_{20}(\Theta,\Phi)\,T_1$$
$$+\frac{2}{35}\sqrt{\frac{2\pi}{15}}[Y_{2-2}(\Theta,\Phi)+Y_{22}(\Theta,\Phi)]\,T_7$$
$$+\frac{64\sqrt{\pi}}{17325}Y_{40}(\Theta,\Phi)\,F_6-\frac{8}{385}\sqrt{\frac{\pi}{10}}[Y_{4-2}(\Theta,\Phi)$$
$$+Y_{42}(\theta,\Phi)]\,F_{12}+\frac{8}{495}\sqrt{\frac{2\pi}{35}}[Y_{4-4}(\Theta,\Phi)+Y_{44}(\Theta,\Phi)]\,F_4$$
$$-\frac{4}{1155}\sqrt{\frac{\pi}{13}}Y_{60}(\Theta,\Phi)\,S_1+\frac{6}{165}\sqrt{\frac{\pi}{1365}}[Y_{6-2}(\Theta,\Phi)$$
$$+Y_{62}(,\Theta\Phi)]\,S_1-\frac{2}{165}\sqrt{\frac{2\pi}{91}}[Y_{6-4}(\Theta,\Phi)+Y_{64}(\Theta,\Phi)]\,S_1$$
$$+\frac{2}{5}\sqrt{\frac{\pi}{3003}}[Y_{6-6}(\Theta,\Phi)+Y_{66}(\Theta,\Phi)]\,S_1$$
$$\langle d_{x^2-y^2}|T_{xx}|d_{xz}\rangle$$
$$=\frac{2}{105}\sqrt{\frac{2\pi}{15}}[Y_{2-1}(\Theta,\Phi)-Y_{21}(\Theta,\Phi)]\,T_{14}$$
$$-\frac{10}{693}\sqrt{\frac{\pi}{5}}[Y_{4-1}(\Theta,\Phi)-Y_{41}(\Theta,\Phi)]\,F_{28}$$
$$+\frac{14}{495}\sqrt{\frac{\pi}{35}}[Y_{4-3}(\Theta,\Phi)-Y_{43}(\Theta,\Phi)]\,F_{10}$$
$$+\frac{4}{165}\sqrt{\frac{2\pi}{273}}[Y_{6-1}(\Theta,\Phi)-Y_{61}(\Theta,\Phi)]\,S_1$$
$$-\frac{6}{55}\sqrt{\frac{\pi}{1365}}[Y_{6-3}(\Theta,\Phi)-Y_{63}(\Theta,\Phi)]\,S_1$$
$$+\frac{2}{15}\sqrt{\frac{\pi}{1001}}[Y_{6-5}(\Theta,\Phi)-Y_{65}(\Theta,\Phi)]\,S_1$$
$$\langle d_{z^2}|T_{xx}|d_{z^2}\rangle$$
$$=-\frac{8\sqrt{\pi}}{1575}Y_{00}(\Theta,\Phi)\,N_1-\frac{4}{105}\sqrt{\frac{\pi}{5}}Y_{20}(\Theta,\Phi)\,T_7$$
$$+\frac{2}{105}\sqrt{\frac{2\pi}{15}}[Y_{2-2}(\Theta,\Phi)+Y_{22}(\Theta,\Phi)]\,T_1$$
$$-\frac{16\sqrt{\pi}}{1925}Y_{40}(\Theta,\Phi)\,F_{12}-\frac{8}{1155}\sqrt{\frac{\pi}{10}}[Y_{4-2}(\Theta,\Phi)$$
$$+Y_{42}(\Theta,\Phi)]\,F_{26}-\frac{8}{385}\sqrt{\frac{\pi}{13}}Y_{60}(\Theta,\Phi)\,S_1$$
$$+\frac{8}{55}\sqrt{\frac{\pi}{1365}}[Y_{6-2}(\Theta,\Phi)+Y_{62}(\Theta,\Phi)]\,S_1$$
$$\langle d_{x^2-y^2}|T_{yx}|d_{xy}\rangle$$
$$=\frac{2}{105}\sqrt{\frac{2\pi}{15}}[Y_{2-2}(\Theta,\Phi)+Y_{22}(\Theta,\Phi)]\,T_{12}$$
$$-\frac{8}{1155}\sqrt{\frac{\pi}{10}}[Y_{4-2}(\Theta,\Phi)+Y_{42}(\Theta,\Phi)]\,F_4$$
$$+\frac{2}{165}\sqrt{\frac{\pi}{1365}}[Y_{6-2}(\Theta,\Phi)+Y_{62}(\Theta,\Phi)]\,S_1$$
$$-\frac{2}{5}\sqrt{\frac{\pi}{3003}}[Y_{6-6}(\Theta,\Phi)+Y_{66}(\Theta,\Phi)]\,S_1$$

$$\langle d_{x^2-y^2}|T_{yx}|d_{yz}\rangle$$
$$=\frac{2}{35}\sqrt{\frac{2\pi}{15}}[Y_{2-1}(\Theta,\Phi)-Y_{21}(\Theta,\Phi)]\,T_4$$
$$-\frac{4}{21}\sqrt{\frac{\pi}{5}}[Y_{4-1}(\Theta,\Phi)-Y_{41}(\Theta,\Phi)]\,F_{21}$$
$$+\frac{4}{165}\sqrt{\frac{\pi}{35}}[Y_{4-3}(\Theta,\Phi)-Y_{43}(\Theta,\Phi)]\,F_{19}$$
$$-\frac{2}{55}\sqrt{\frac{\pi}{1365}}[Y_{6-3}(\Theta,\Phi)-Y_{63}(\Theta,\Phi)]\,S_1$$
$$-\frac{2}{15}\sqrt{\frac{\pi}{1001}}[Y_{6-5}(\Theta,\Phi)-Y_{65}(\Theta,\Phi)]\,S_1$$

$$\langle d_{x^2-y^2}|T_{xx}|d_{Z^2}\rangle$$
$$=\frac{-8\sqrt{3\pi}}{1575}Y_{00}(\Theta,\Phi)\,N_1+\frac{4}{315}\sqrt{\frac{3\pi}{5}}Y_{20}(\Theta,\Phi)\,T_{10}$$
$$-\frac{2}{315}\sqrt{\frac{2\pi}{5}}[Y_{2-2}(\Theta,\Phi)+Y_{22}(\Theta,\Phi)]\,T_{10}$$
$$-\frac{64\sqrt{3\pi}}{17325}Y_{40}(\Theta,\Phi)\,F_{23}+\frac{8}{3465}\sqrt{\frac{3\pi}{10}}[Y_{4-2}(\Theta,\Phi)$$
$$+Y_{42}(\Theta,\Phi)]\,F_1-\frac{8}{495}\sqrt{\frac{6\pi}{35}}[Y_{4-4}(\Theta,\Phi)+Y_{44}(\Theta,\Phi)]F_{19}$$
$$+\frac{4}{1155}\sqrt{\frac{3\pi}{13}}Y_{60}(\Theta,\Phi)\,S_1-\frac{8}{165}\sqrt{\frac{\pi}{455}}[Y_{6-2}(\Theta,\Phi)$$
$$+Y_{62}(\Theta,\Phi)]\,S_1+\frac{2}{165}\sqrt{\frac{6\pi}{91}}[Y_{6-4}(\Theta,\Phi)+Y_{64}(\Theta,\Phi)]\,S_1$$

$$\langle d_{x^2-y^2}|T_{zz}|d_{x^2-y^2}\rangle$$
$$=\frac{-16\sqrt{\pi}}{1575}Y_{00}(\Theta,\Phi)\,N_1+\frac{8}{315}\sqrt{\frac{\pi}{5}}Y_{20}(\Theta,\Phi)\,T_1$$
$$-\frac{128\sqrt{\pi}}{17325}Y_{40}(\Theta,\Phi)\,F_6-\frac{16}{495}\sqrt{\frac{2\pi}{35}}[Y_{4-4}(\Theta,\Phi)$$
$$+Y_{44}(\Theta,\Phi)]\,F_4+\frac{8}{1155}\sqrt{\frac{\pi}{13}}Y_{60}(\Theta,\Phi)\,S_1$$
$$+\frac{4}{165}\sqrt{\frac{2\pi}{91}}[Y_{6-4}(\Theta,\Phi)+Y_{64}(\Theta,\Phi)]\,S_1$$

$$\langle d_{z^2}|T_{zz}|d_{z^2}\rangle$$
$$=\frac{16\sqrt{\pi}}{1575}Y_{00}(\Theta,\Phi)\,N_1+\frac{8}{105}\sqrt{\frac{\pi}{5}}Y_{20}(\Theta,\Phi)\,T_7$$
$$+\frac{32\sqrt{\pi}}{1925}Y_{40}(\Theta,\Phi)\,F_{12}+\frac{16}{385}\sqrt{\frac{\pi}{13}}Y_{60}(\Theta,\Phi)\,S_1$$

$$\langle d_{x^2-y^2}|T_{zz}|d_{xz}\rangle$$
$$=-\frac{4}{105}\sqrt{\frac{2\pi}{15}}[Y_{2-1}(\Theta,\Phi)-Y_{21}(\Theta,\Phi)]\,T_4$$
$$+\frac{4}{495}\sqrt{\frac{\pi}{5}}[Y_{4-1}(\Theta,\Phi)-Y_{41}(\Theta,\Phi)]\,F_{18}$$
$$-\frac{4}{495}\sqrt{\frac{\pi}{35}}[Y_{4-3}(\Theta,\Phi)-Y_{43}(\Theta,\Phi)]\,F_4$$
$$-\frac{4}{165}\sqrt{\frac{2\pi}{273}}[Y_{6-1}(\Theta,\Phi)-Y_{61}(\Theta,\Phi)]\,S_1$$
$$+\frac{8}{55}\sqrt{\frac{\pi}{1365}}[Y_{6-3}(\Theta,\Phi)-Y_{63}(\Theta,\Phi)]\,S_1$$

$$\langle d_{z^2}|T_{zz}|d_{x^2-y^2}\rangle$$
$$=\frac{4}{315}\sqrt{\frac{2\pi}{5}}[Y_{2-2}(\Theta,\Phi)+Y_{22}(\Theta,\Phi)]\,T_{10}$$
$$-\frac{16}{3465}\sqrt{\frac{3\pi}{10}}[Y_{4-2}(\Theta,\Phi)+Y_{42}(\Theta,\Phi)]\,F_1$$
$$+\frac{16}{165}\sqrt{\frac{\pi}{455}}[Y_{6-2}(\Theta,\Phi)+Y_{62}(\Theta,\Phi)]\,S_1$$

$$\langle d_{xz}|T_{xz}|d_{x^2-y^2}\rangle$$
$$=\frac{2\sqrt{2\pi}}{525}Y_{00}(\Theta,\Phi)\,N_1+\frac{2}{105}\sqrt{\frac{2\pi}{5}}Y_{20}(\Theta,\Phi)\,T_4$$
$$+\frac{2}{105}\sqrt{\frac{\pi}{5}}[Y_{2-2}(\Theta,\Phi)+Y_{22}(\Theta,\Phi)]\,T_9$$
$$-\frac{2\sqrt{2\pi}}{825}Y_{40}(\Theta,\Phi)\,F_2+\frac{2}{231}\sqrt{\frac{\pi}{5}}[Y_{4-2}(\Theta,\Phi)+$$
$$+Y_{42}(\Theta,\Phi)]\,F_{22}+\frac{2}{165}\sqrt{\frac{\pi}{35}}[Y_{4-4}(\Theta,\Phi)+Y_{44}(\Theta,\Phi)]\,F_4$$
$$+\frac{4}{1155}\sqrt{\frac{2\pi}{13}}Y_{60}(\Theta,\Phi)\,S_1-\frac{8}{165}\sqrt{\frac{2\pi}{1365}}[Y_{62}(\Theta,\Phi)$$
$$+Y_{62}(\Theta,\Phi)]\,S_1+\frac{4}{165}\sqrt{\frac{\pi}{91}}[Y_{6-4}(\Theta,\Phi)+Y_{64}(\Theta,\Phi)]\,S_1$$

$$\langle d_{x^2-y^2}|T_{yy}|d_{x^2-y^2}\rangle$$
$$=\frac{8\sqrt{\pi}}{1575}Y_{00}(\Theta,\Phi)\,N_1-\frac{4}{315}\sqrt{\frac{\pi}{5}}Y_{20}(\Theta,\Phi)\,T_1$$
$$-\frac{2}{35}\sqrt{\frac{2\pi}{15}}[Y_{2-2}(\Theta,\Phi)+Y_{22}(\Theta,\Phi)]\,T_7$$
$$+\frac{64\sqrt{\pi}}{17325}Y_{40}(\Theta,\Phi)\,F_6+\frac{8}{385}\sqrt{\frac{\pi}{10}}[Y_{4-2}(\Theta,\Phi)$$
$$+Y_{42}(\Theta,\Phi)]\,F_{12}+\frac{8}{495}\sqrt{\frac{2\pi}{35}}[Y_{4-4}(\Theta,\Phi)+Y_{44}(\Theta,\Phi)]\,F_4$$
$$-\frac{4}{1155}\sqrt{\frac{\pi}{13}}Y_{60}(\Theta,\Phi)\,S_1-\frac{6}{165}\sqrt{\frac{\pi}{1365}}[Y_{6-2}(\Theta,\Phi)$$
$$+Y_{62}(\Theta,\Phi)]\,S_1-\frac{2}{165}\sqrt{\frac{2\pi}{91}}[Y_{6-4}(\Theta,\Phi)+Y_{64}(\Theta,\Phi)]S_1$$
$$-\frac{2}{5}\sqrt{\frac{\pi}{3003}}[Y_{6-6}(\Theta,\Phi)+Y_{66}(\Theta,\Phi)]\,S_1$$

$$\langle d_{x^2-y^2}|T_{yy}|d_{x^2}\rangle$$
$$=-\frac{2}{105}\sqrt{\frac{2\pi}{15}}[Y_{2-1}(\Theta,\Phi)-Y_{21}(\Theta,\Phi)]\,T_{10}$$
$$+\frac{2}{315}\sqrt{\frac{\pi}{5}}[Y_{4-1}(\Theta,\Phi)-Y_{41}(\Theta,\Phi)]\,F_{29}$$
$$-\frac{2}{99}\sqrt{\frac{\pi}{35}}[Y_{4-3}(\Theta,\Phi)-Y_{43}(\Theta,\Phi)]\,F_{16}$$
$$-\frac{2}{55}\sqrt{\frac{\pi}{1365}}[Y_{6-3}(\Theta,\Phi)-Y_{63}(\Theta,\Phi)]\,S_1$$
$$-\frac{2}{15}\sqrt{\frac{\pi}{1001}}[Y_{6-5}(\Theta,\Phi)-Y_{65}(\Theta,\Phi)]\,S_1$$

$$\langle d_{z^2}|T_{yy}|d_{x^2-y^2}\rangle$$
$$=\frac{8\sqrt{3\pi}}{1575}Y_{00}(\Theta,\Phi)\,N_1-\frac{4}{315}\sqrt{\frac{3\pi}{5}}Y_{20}(\Theta,\Phi)\,T_{10}$$
$$-\frac{2}{315}\sqrt{\frac{2\pi}{5}}[Y_{2-2}(\Theta,\Phi)+Y_{22}(\Theta,\Phi)]\,T_{10}$$
$$+\frac{64\sqrt{3\pi}}{17325}Y_{40}(\Theta,\Phi)\,F_{23}+\frac{8}{3465}\sqrt{\frac{3\pi}{10}}[Y_{4-2}(\Theta,\Phi)$$
$$+Y_{42}(\Theta,\Phi)]\,F_1+\frac{8}{495}\sqrt{\frac{6\pi}{35}}[Y_{4-4}(\Theta,\Phi)+Y_{44}(\Theta,\Phi)]\,F_{19}$$
$$-\frac{4}{1155}\sqrt{\frac{3\pi}{13}}Y_{60}(\Theta,\Phi)\,S_1-\frac{8}{165}\sqrt{\frac{\pi}{455}}[Y_{6-2}(\Theta,\Phi)$$
$$+Y_{62}(\Theta,\Phi)]\,S_1-\frac{2}{165}\sqrt{\frac{6\pi}{91}}[Y_{6-4}(\Theta,\Phi)+Y_{64}(\Theta,\Phi)]\,S_1$$

$$\langle d_{z^2}|T_{yy}|d_{z^2}\rangle$$
$$=-\frac{8\sqrt{\pi}}{1575}Y_{00}(\Theta,\Phi)\,N_1-\frac{4}{105}\sqrt{\frac{\pi}{5}}Y_{20}(\Theta,\Phi)\,T_7$$
$$-\frac{2}{105}\sqrt{\frac{2\pi}{15}}[Y_{2-2}(\Theta,\Phi)+Y_{22}(\Theta,\Phi)]\,T_1$$
$$-\frac{16\sqrt{\pi}}{1925}Y_{40}(\Theta,\Phi)\,F_{12}+\frac{8}{1155}\sqrt{\frac{\pi}{10}}[Y_{4-2}(\Theta,\Phi)$$
$$+Y_{42}(\Theta,\Phi)]\,F_{26}-\frac{8}{385}\sqrt{\frac{\pi}{13}}Y_{60}(\Theta,\Phi)\,S_1$$
$$-\frac{8}{55}\sqrt{\frac{\pi}{1365}}[Y_{6-2}(\Theta,\Phi)+Y_{62}(\Theta,\Phi)]\,S_1$$

$$\langle d_{yz}|T_{yz}|d_{x^2-y^2}\rangle$$
$$=-\frac{2\sqrt{2\pi}}{525}Y_{00}(\Theta,\Phi)\,N_1-\frac{2}{105}\sqrt{\frac{2\pi}{5}}Y_{20}(\Theta,\Phi)\,T_4$$
$$+\frac{2}{105}\sqrt{\frac{\pi}{15}}[Y_{2-2}(\Theta,\Phi)+Y_{22}(\Theta,\Phi)]\,T_9$$
$$+\frac{2\sqrt{2\pi}}{825}Y_{40}(\Theta,\Phi)\,F_2+\frac{2}{231}\sqrt{\frac{\pi}{5}}[Y_{4-2}(\Theta,\Phi)$$
$$+Y_{42}(\Theta,\Phi)]\,F_{22}-\frac{2}{165}\sqrt{\frac{\pi}{35}}[Y_{4-4}(\Theta,\Phi)+Y_{44}(\Theta,\Phi)]\,F_4$$
$$-\frac{4}{1155}\sqrt{\frac{2\pi}{13}}Y_{60}(\Theta,\Phi)\,S_1-\frac{8}{165}\sqrt{\frac{2\pi}{1365}}[Y_{6-2}(\Theta,\Phi)$$
$$+Y_{62}(\Theta,\Phi)]\,S_1-\frac{4}{165}\sqrt{\frac{\pi}{91}}[Y_{6-4}(\Theta,\Phi)+Y_{64}(\Theta,\Phi)]\,S_1$$

$$\langle d_{xy}|T_{zy}|d_{z^2}\rangle$$
$$=\frac{4}{105}\sqrt{\frac{2\pi}{5}}[Y_{2-1}(\Theta,\Phi)-Y_{21}(\Theta,\Phi)]\,T_4$$
$$+\frac{2}{165}\sqrt{\frac{\pi}{15}}[Y_{4-1}(\Theta,\Phi)-Y_{41}(\Theta,\Phi)]\,F_{25}$$
$$+\frac{2}{165}\sqrt{\frac{\pi}{105}}[Y_{4-3}(\Theta,\Phi)-Y_{43}(\Theta,\Phi)]\,F_{24}$$
$$-\frac{2}{165}\sqrt{\frac{2\pi}{91}}[Y_{6-1}(\Theta,\Phi)-Y_{61}(\Theta,\Phi)]\,S_1$$
$$-\frac{4}{55}\sqrt{\frac{\pi}{455}}[Y_{6-3}(\Theta,\Phi)-Y_{63}(\Theta,\Phi)]\,S_1$$

$$\langle d_{yz}|T_{zy}|d_{z^2}\rangle$$
$$=\frac{4}{525}\sqrt{\frac{\pi}{3}}Y_{00}(\Theta,\Phi)\,N_1+\frac{4}{105}\sqrt{\frac{\pi}{15}}Y_{20}(\Theta,\Phi)\,T_{11}$$
$$+\frac{2}{105}\sqrt{\frac{2\pi}{5}}[Y_{2-2}(\Theta,\Phi)+Y_{22}(\Theta,\Phi)]\,T_4$$
$$-\frac{8}{5775}\sqrt{\frac{\pi}{3}}Y_{40}(\Theta,\Phi)\,F_{24}-\frac{4}{165}\sqrt{\frac{\pi}{30}}[Y_{4-2}(\Theta,\Phi)$$
$$+Y_{42}(\Theta,\Phi)]\,F_{25}-\frac{16}{385}\sqrt{\frac{\pi}{39}}Y_{60}(\Theta,\Phi)\,S_1$$
$$-\frac{16}{165}\sqrt{\frac{\pi}{455}}[Y_{6-2}(\Theta,\Phi)+Y_{62}(\Theta,\Phi)]\,S_1$$

$$\langle d_{xy}|T_{zy}|d_{z^2}\rangle$$
$$=-\frac{8\sqrt{3\pi}}{1575}Y_{00}(\Theta,\Phi)\,N_1+\frac{4\sqrt{15\pi}}{1575}Y_{20}(\Theta,\Phi)\,T_{10}$$
$$-\frac{64\sqrt{3\pi}}{17325}Y_{40}(\Theta,\Phi)\,F_{23}+\frac{8}{495}\sqrt{\frac{6\pi}{35}}[Y_{4-4}(\Theta,\Phi)$$
$$+Y_{44}(\Theta,\Phi)]\,F_{19}+\frac{12}{3465}\sqrt{\frac{3\pi}{13}}Y_{60}(\Theta,\Phi)\,S_1$$
$$-\frac{6}{495}\sqrt{\frac{6\pi}{91}}[Y_{6-4}(\Theta,\Phi)+Y_{64}(\Theta,\Phi)]\,S_1$$

References

(1) R. M. Golding, *Pure Appl. Chem.*, **32**, 123 (1972)
(2) R. M. Golding and M. P. Halton, *Aust. J. Chem.*, **25**, 2577 (1972)
(3) R. M. Golding and P. Pyykko, *Mol. Phys.*, **26**, 1389 (1973)
(4) R. M. Golding, R. O. Pascual and J. Vrbncich, *Mol. Phys.*, **31**, 731 (1976)
(5) H. M. McConnell and R. E. Robertson, *J. Chem. Phys.*, **29**, 1361 (1958)
(6) R. J. Kurland and B. R. McGravey, *J. Magn. Res.*, **2**, 286 (1970)
(7) A. D. Buckingham and P.J. Stiles, *Mol. Phys.*, **24**, 99 (1972)
(8) P. J. Stiles, *Mol Phys.*, **27**, 501 (1974); P. J. Stiles, *Mol. Phys*, **29**, 1271 (1975); R. M. Golding and L. C. Stubbs, Proc. R. Soc., **A354**, 223 (1977)
(9) R. M. Golding, R. O. Pascual and S. Ahn, *J. Magn, Res.*, **46**, 406 (1982)
(10) C. J. Ballhausen, "Introduction to Ligand Field Theory", McGraw Hill, 1962.
(11) J. S. Griffth, "The Theory of Transition - Metal Ions". Cambridge Univ. Press, 1961.
(12) A. D. McConnel and Strathdee, *Mol. Phys* **2**, 129 (1959)
(13) R. M. Pitzer, C. W. Kein and W. N. Lipscomb, *J. Chem. Phys*, **37**, 267 (1962)
H. M. McConnel and R. E. Robertson, **29**, 1361 (1958)
(14) B. Bleaney *J. Magn. Res*, **8**, 91 (1972)
(15) N. Moshinsky, *Nucl. Phys*, **13**, 104 (1959)
(16) L. C. Stubbs, Unpublished Thesis (Ph D, the University of New South Wales, 1978)
(17) M. Rotenberg, "3-j and 6-j Symbols". The Technology Press, Cambridge, 1959.
(18) A. R. Edmonds, "Angular Momentum in Quantum Mechanics", Princeton University Press, 1957.
(19) R. M. Golding and J. R. Mcdonald, *Mol. Phys*. **31**, 28 (1975)
(20) R. M. Golding and L. C. Stubbs, *J. Magn. Res*, **33**, 627 (1979)